Effects of irradiation on mechanical properties of nuclear UO2 fuels evaluated by Vickers indentation at room temperature

I. Zacharie-Aubrun, R. Henry, Th. Blay, L. Brunaud, J. M. Gatt, J. Noirot, S. Meille

Effects of irradiation on mechanical properties of nuclear UO_2 fuels evaluated by Vickers indentation at room temperature

I. Zacharie-Aubrun[1], R. Henry[1,2], Th. Blay[1], L. Brunaud[1], JM. Gatt[1], J. Noirot[1], S. Meille[2]

[1]CEA, DES, IRESNE, DEC, Cadarache F-13108 Saint-Paul-Lez-Durance, France

[2]Univ Lyon, INSA-Lyon, MATEIS CNRS UMR 5510, 69621 Villeurbanne, France

Highlights:

- Irradiation effect on hardness and apparent fracture toughness of UO_2 fuels was studied using a large number of Vickers tests.
- The Vickers hardness of UO_2 quickly increased with the local burnup but decreased when the fuel restructured into the HBS.
- The Vickers fracture toughness of the non-restructured doped UO_2 increased quickly during the first irradiation cycle but was then constant with increasing local burnup. In the HBS, the fracture toughness was shown to be difficult to determine from indentation tests.

Abstract:

Vickers indentation was used to evaluate the hardness and the apparent fracture toughness of unirradiated and irradiated UO_2 fuels, with the objective to determine the effects of the irradiation on mechanical properties. Indentation tests were realized at room temperature on standard and doped UO_2 fuels, irradiated in a pressurised water reactor up to a burnup of 81.6 GWd/tM. For the highest burnups, the fuels had restructured in a high burnup structure (HBS) on the periphery of the pellets.

More than 100 valid impressions for the Vickers hardness determination were obtained on each fuel. The Vickers hardness of both UO_2 increased with the local burnup, due to irradiation defects such as dislocations and fission products but decreased when the fuel restructured into the HBS.

Valid crack patterns for the Vickers fracture toughness were only obtained for indentations inside the large grains of irradiated doped UO_2 fuels or for both restructured fuels. The Vickers fracture toughness of the non-restructured doped UO_2 was shown to increase quickly during the first irradiation cycle but was then constant with increasing local burnup. This increase of the apparent fracture toughness was mainly due to the decrease of the crack length from the corner of the indents, attributed to the interactions of the cracks with the defects such as bubbles or fission product precipitates and associated residual stresses. In the HBS, short cracks from the corner of the indents that followed grain boundaries of small grains led to high fracture toughness values. However, the use of the literature equations to calculate the apparent fracture toughness on porous samples such as HBS is questioned. All tests clearly illustrated the weakness of the grain boundaries in irradiated fuels.

Key words: brittle, fracture toughness, hardness, irradiated nuclear fuel, doped UO_2, UO_2, HBS, indentation, Vickers, nuclear, mechanical properties, grain boundaries, storage, spent fuel, alpha decay

Abrevations:

ECD: Equivalent Circle Diameter
EPMA: Electron Probe Micro Analysis
FIB: Focused Ion Beam
HBS: High Burnup Structure
LOCA: Loss of coolant accident
LWR: Light Water Reactor
OM: Optical Microscopy
PWR: Pressurized Water Reactor

RIA: Reactivity initiated accident
SEM: Scanning Electron Microscope
SENB-S: Single Edge Notched Bending-Saw

1. INTRODUCTION

During the operation of the PWR reactors, chemical and physical properties of the nuclear fuel are modified by the effects of irradiation [1]. Concerning the brittle mechanical properties of the fuel, macroscopic data have been acquired, for unirradiated fuels, by 3 points bending tests [2][3]. For irradiated fuels, no macroscopic data are available because appropriate samples for conventional mechanical tests are not achievable due to fragmentation by the cracks formed during irradiation.
To collect data on the mechanical properties of irradiated fuels, testing at a local scale is thus necessary. Knowing the mechanical properties of the fuels at a microscopic scale is important to model the behaviour of the fuel under irradiation in normal condition, but also the fuel fragmentation and pulverization during reactivity initiated accident (RIA) [4][5] and loss of coolant accidents (LOCA) [6][7][8].
Vickers indentation tests were already used to evaluate the local hardness and fracture toughness of unirradiated [9] and irradiated fuels [10]. More recently, Frazer *et al.* performed micro mechanical bending tests on unirradiated UO_2 fuel [11]. At room temperature, they measured fracture stresses of unirradiated UO_2 in a porous poly-crystal and in a dense mono-crystal. Henry *et al.* carried out similar micro-mechanical tests on unirradiated fuels and on irradiated UO_2 fuels at a burnup of about 35 GWd/tM, in order to determine their local fracture properties [12][13][14]. Finally, only few results are available in literature on the local mechanical properties of unirradiated and irradiated fuels.
The goal of this paper is to use Vickers indentation to measure the hardness and the local apparent fracture toughness of different fuels, with standard and large grains, irradiated up to a high burnup of 81.6 GWd/tM, in the objective to determine the effects of the irradiation on brittle mechanical properties of nuclear UO_2 fuels. The results obtained by Vickers indentation technique, still debated regarding its capability to estimate the absolute fracture toughness [15][16], will be discussed. The results will be compared with the local measurements available in the literature.

2. MATERIALS AND PREPARATION

The fuel samples used in this work were unirradiated and irradiated UO_2, with standard grain size (about 10 µm), hereafter referred as standard UO_2 and large grain size (about 60 µm) obtained by the addition of Cr_2O_3 before pressing and sintering, hereafter referred as doped UO_2.
Irradiated fuels were taken from fuel rods irradiated in a PWR for several cycles. Different burnups were selected up to an average burnup of the pellet of 81.6 GWd/tM. As a consequence of thermal and burn-up gradients between the pellet centreline and the periphery of the irradiated pellet, the microstructure of the fuel varies along the pellet radius. This evolution is mainly visible for high burnup fuels (Fig. 1 and Fig. 3).

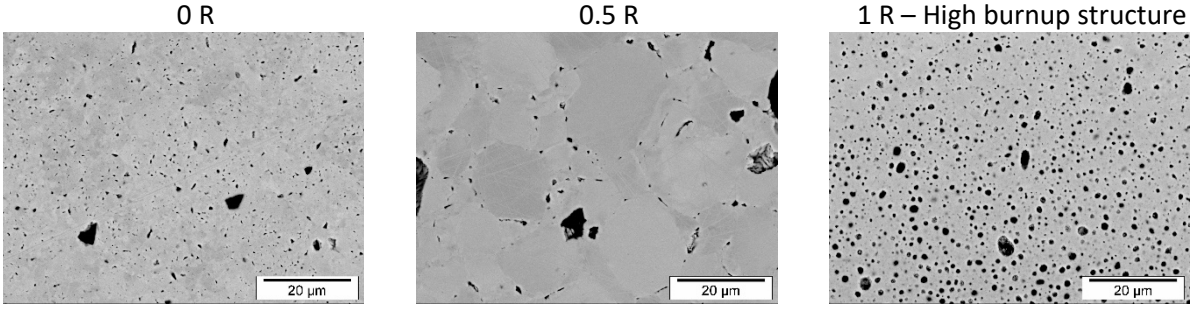

Fig. 1. Micrographs of the microstructure of an irradiated standard UO_2 fuel – 73 GWd/tM at different radial positions on the polished cross section (R pellet radius). In the centre of the pellet (0 R), the micrograph shows a microstructure with fission gas bubbles located on the grains boundaries (inter-granular) and inside the grains (intra-granular) [17]. At 0.5 R, the bubbles are mainly located on grains boundaries. On the periphery of the pellet (rim zone), the fuel is restructured into HBS with a subdivision in sub-micrometre grains and with many micrometric bubbles [10][18]

In the centre of the pellet (0R), the micrographs (Fig. 1-0R and Fig. 3-0R) show a microstructure with fission gas bubbles located on the grains boundaries (inter-granular) and inside the grains (intra-granular) [17]. At 0.5 R, the bubbles are mainly located on grains boundaries (Fig. 1-0.5R and Fig. 3-0.5R. On the periphery of the pellet (rim zone, Fig. 1-1R and Fig. 3-1R), the fuel is restructured into HBS with a subdivision in sub-micrometre grains and with many micrometric bubbles (Fig. 2) [10] [18]**.**

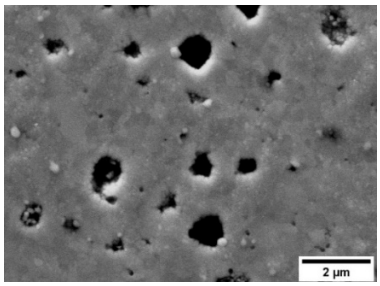

Fig. 2. SEM micrograph of HBS – Doped UO_2 fuel – 60.8 GWd/tM

The initial porosity of the fuels varied between 3.1 and 5.4 % for both standard and doped fuels (Table 2). The porosity of the fuels up to an average burnup of the pellet of 38 GWd/tM was evaluated using apparent density measurements by immersion in bromobenzene, considering a theoretical density for a fully dense material corrected from the solid swelling of 0.64%/10 GWd/tM [18]. The porosity of the high burnups fuels (outside the HBS zone) was evaluated by SEM images analysis and averaged from the centre to the intermediate zone. The local burnup was determined from the neodymium content measured by EPMA. On the periphery (rim zone) of the pellets, where the local burnup is the highest and where the fuel is restructured into HBS, the local porosity fraction of the fuels was measured on each high burnup sample of respectively an average pellet burnup of 60.8, 72.2 and 81.6 GWd/tM, using SEM images analysis. The porosity varied between 6 and 15 % [10][19]. For each high burnup sample, the porosity range is given in the Table 2.

The initial U^{235} enrichment was between 3.7 and 4.5 %. The doping of the UO_2 fuel with Cr_2O_3 was between 0.16 wt% and 0.2 wt%.

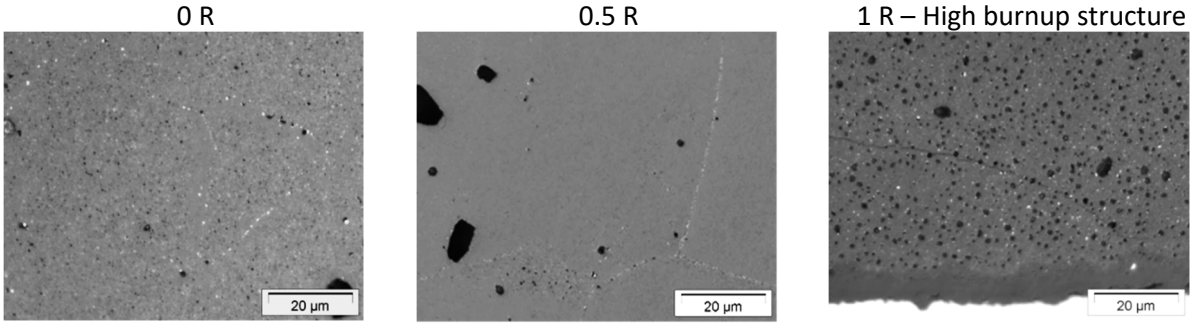

Fig. 3. Micrographs of the microstructure of an irradiated doped UO_2 fuel – 61 GWd/tM at different radial positions on the polished cross section (R pellet radius).

The older spent fuel was an UO_2 - 38 GWd/tM stored during nearly 18 years (6449 days). The storage times of other UO_2 samples after irradiation in reactor were between a bit more than 2 years (791 days) and more than 5 years (1947 days).The high burnup fuels have a storage time between 791 days and 1156 days.

The main sample characteristics of the fuels are given in Table 2. Detailed post irradiation examinations of several of these fuels can also be found in [18].The fuel rods were irradiated at average linear powers between 112 and 278 W/cm (Table 1). Two fuels present an increment of power in the second cycle linked to a displacement of the assembly towards the centre of the reactor heart. Under the effect of exhaustion of the fuel, the average power then tends to decrease over time. The mean linear powers during the last cycle of all high burnup fuels were similar and about 155 W/cm.

Table 1: Mean linear power (W/cm) of the studied fuel samples for each reactor cycle

	Cycle 1	Cycle 2	Cycle 3	Cycle 4	Cycle 5	Cycle 6	Cycle 7
UO_2 - 15.6 GWd/tM	**263**						
UO_2 - 32.8 GWd/tM	190	**191**					
UO_2 - 38 GWd/tM	218	256	214				
UO_2 - 72.2 GWd/tM	194	112	200	183	159	**154**	
UO_2 - 81.6 GWd/tM	158	179	213	197	187	182	**155**
Doped UO_2 - 16.5 GWd/tM	**278**						
Doped UO_2 - 35.4 GWd/tM	203	**202**					
Doped UO_2 - 60.8 GWd/tM	225	256	206	193	**154**		

Indentation testing requires a high quality of sample surface. Radial or longitudinal sections of the various fuels were embedded under vacuum in an epoxy resin. The surface was grinded with abrasive papers and polished with a series of diamond pastes down to 1 µm. The final polishing step was done with a colloidal solution of silica (0.04 µm).

*Table 2: Samples characteristics of PWR fuels. The closed porosity fraction of the unirradiated and irradiated fuels up to an average burnup of the pellet of 38 GWd/tM was evaluated using density measurements determined by immersion in bromobenzene as a percentage of the theoretical value for fully dense material and corrected from the solid swelling of 0.64%/10 GWd/tM [18]. The porosity of the high burnups fuels (out of the HBS) was evaluated by SEM images analysis. Out of the HBS, the porosity fraction was averaged from the centre to the intermediate zone. In the HBS, the porosity fraction was the local measurement. Fuels, coming from the same batch, are marked with (*1) or (*2). Grain size was measured by a mean linear intercept method [20].*

Fuel	Average burnup of the pellet (GWd/tM)	Average grain size (µm)	Porosity fraction (%)	Storage time after irradiation (days)
Standard UO_2	0	10	5.0	0
Standard UO_2	0	12	3.8	0
Standard UO_2	0	11	4.8	0
Standard UO_2	15.6	11	3.5	1947
Standard UO_2	32.8	9	3.2	821
Standard UO_2	38	15	4.7	6449
Standard UO_2 – Out of rim (*1)	72.2	10	7.2	1156
Standard UO_2 – Rim (*1)	72.2	<1	7.8 to 14	1156
Standard UO_2 – Out of rim (*1)	81.6	10	8.1	1125
Standard UO_2 – Rim (*1)	81.6	<1	8.5 to 15	1125
Doped UO_2 (*2)	0	62	5.0	0
Doped UO_2	0	55	3.1	0
Doped UO_2 (*2)	16.5	62	4.3	1947
Doped UO_2	35.4	55	3.1	1035
Doped UO_2 – Out of rim (*2)	60.8	62	5.1	791
Doped UO_2 – Rim (*2)	60.8	<1	6 to 12.2	791

3. METHODS

In the Vickers indentation technique, a pyramidal tip with an apex angle θ of 68°, is applied at a load *P* on the sample surface, leaving a squared residual impression. With the mean impression diagonal length 2*a*, the Vickers hardness (*HV*) of the material is given by the ratio of the applied load on the contact area:

$$H_V = P.\sin\theta/(2.a^2) \quad \text{(Eq. 1)}$$

For sufficiently high applied loads, four cracks are generated from the corners of the residual impression after unloading. The propagation of these cracks stops when the residual stress intensity factor at the tip of each crack is lower than the fracture toughness of the material.
It has to be noted that Vickers indentation testing brings only an estimation of an apparent fracture toughness rather than accurate measurements [16], notably due to the difficulty to verify if the assumptions behind the equations are satisfied.
The morphology of the cracks depends on the indentation load, the tip geometry and the toughness of the material. Half penny (median) or Palmqvist (radial) cracks are the most common crack configurations in brittle materials (Fig. 4). Palmqvist mode forms at low loads. Transition between Palmqvist and Half penny configuration usually takes place when the indentation load increases.

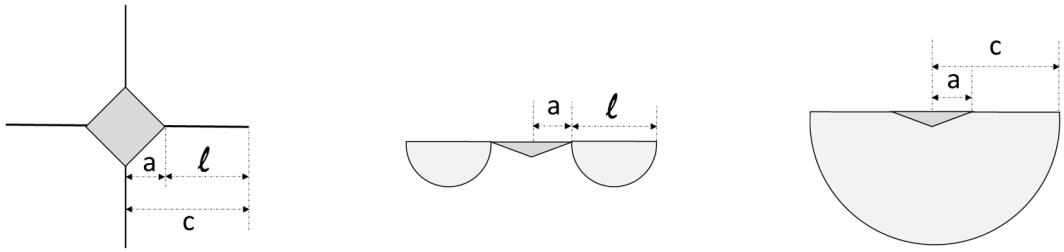

Vickers impression and cracks Palmqvist mode Half penny mode

Fig. 4. Morphology of the cracks by Vickers indentation

Several equations (Table 3) are available to determine the fracture toughness K_c by indentation, both in the Half penny mode and in the Palmqvist mode. These depend on the Young's modulus E, the projected contact hardness H, the applied load P, the half diagonal of the indent a and the crack length, l or c (Fig. 4). Different authors showed that the Palmqvist mode was found for $c/a < 2$ and the Half penny mode for $c/a > 2.5$ [25][28]. For each mode, equations have different coefficients of calibration and can therefore give different results for a given set of parameters. One issue is therefore to choose the appropriate equation for the material of interest.
The Young's modulus at ambient temperature of unirradiated and irradiated UO_2 was calculated with the expression: *E (GPa) = 221.5 (1-2.62 p)*, where *p* is the porosity fraction (Table 2). This expression from Gatt *et al.* [22] is used in the thermo-mechanical code ALCYONE [21]. This code simulates the influence of burnup on Young's modulus through the evolution of porosity fraction during irradiation. The calculated values of Young's modulus are similar to the experimental values proposed by Marchetti *et al*. [23] and are needed to calculate the apparent fracture toughness from indentation tests.
For Half penny cracks in Vickers indentation, the most common equation is the one proposed by Anstis *et al.* (Table 3 – Eq.1), valid for $c/a \geq 2$. Anstis *et al.* have calibrated the equation with conventional tests (notched samples of well-controlled geometry) on reference monocrystalline and polycrystalline ceramics. They showed a good consistency between the measured fracture toughness between indentation and conventional tests. Other authors showed that the equation of Niihara gives reliable results for $c/a > 2$ (Fig. 5) in several ceramics [25][28]. Cubic zirconia 8Y-FSZ (stabilized with 8 mol% of Yttrium) was already tested by Vickers indentation between 100 mN and 660 mN [12]. This ceramic is a relevant model material of the UO_2 fuel since it has close fracture properties and a similar microstructure [12]. For a ratio $c/a > 2$, the fracture toughness given by the equation of Niihara *et al.* in Half penny mode (Table 3 – Eq.2) is consistent with macroscopic or microscopic measurements, obtained by conventional mechanical tests [25][28].
To calculate the apparent fracture toughness of nuclear UO_2 fuel by Vickers indentation, the equation of Niihara for Half penny mode (Table 3 – Eq.2) will be used [12]. The results will be also proposed with the equations of Anstis (Table 3 – Eq.1) and Matzke (Table 3 – Eq.5) to compare our

results with the literature. In the HBS, as explained in section 4.3, the equation of Niihara for Palmqvist mode (Table 3 – Eq.4) will be preferred.

In this work, Vickers indentation was performed with an optical microscope (Olympus, Tokyo, Japan) set in a shielded cell and operated at room temperature. The micro-indenter (Anton-Paar, Graz, Austria), equipped with a Vickers diamond tip, was set instead one of the microscope objectives. The applied load varied between 0.1 and 2 N and was calibrated with calibrated weights. Images were acquired with a F-view camera with 1030x1300 pixels. The pixel size was calibrated with a certificated stage micrometre (1 mm-100 steps). The measurements were realized using the Olympus Soft Imaging System software.

Table 3: Equations for the determination of fracture toughness by Vickers indentation

Author	Crack mode	Eq. n°	Equation	Parameters
Anstis [24]	Half penny $2 \leq c/a$	1	$K_{1c} = (0{,}016 \pm 0.004) * \left(\frac{E}{H}\right)^{\frac{1}{2}}$	
Niihara [25]	Half penny $2.5 \leq c/a$	2	K_{1c}	*E* : Young's modulus *H* : Contact hardness
Laugier [26]	Palmqvist	3	$K_{1c} = 0{,}015 * \left(\frac{a}{l}\right)^{\frac{1}{2}} * \left(\frac{E}{H}\right)^{\frac{2}{3}}$	H P
Niihara [25]	Palmqvist $0.25 \leq l/a \leq 2.5$	4	$K_{1c} = 0.0089 * \left(\frac{E}{\sin 68° \; H}\right)^{\frac{2}{5}} * \left(\frac{P}{a \; l^{1/2}}\right)$	*P* : Load *a* : Mean half diagonal of the indent *l* : Mean length of the crack *c= l+a (see Figure 2)*
Matzke [10]		5	K_{1c}	
Casellas [27]	Palmqvist	6	K_{1c}	

The indentation tests were performed at room temperature with the following parameters: applied load of 0.735 N (75 gf), acquisition time of 10 s and loading rate of 10 gf.s^{-1}, as required in Vickers standard test methods ASTM C1327 [29] and ISO [30][31]. The choice of the 0.735 N load was determined on unirradiated fuels and was the best compromise between valid impressions and the precision of impression diagonal measurements with the optical microscope: indeed, above 100 g, presence of spalling and non-straight cracks was noted and below 50 g the impressions were too small to be properly imaged. For each sample, indentations were performed at different local radial positions from the centre to the periphery of the pellet, with around 10 impressions for each radial position.

Acceptable indentations were determined as required in ASTM C1327 [29] and ISO [30][31]. A first visual selection eliminated unreliable impressions because of spalled edges or pores. The impressions had also to be squared with a difference between the lengths of the two diagonals lower than 5%. To determine valid indentation crack pattern, the four cracks at the impression corners had to be straight, parallel to the axis of the diagonals. The indentations with cracked grain boundaries around the impression were also eliminated. A statistic sorting was also applied: the measurements of the average diagonal 2a and the average crack length of indentations c were removed if they were out of the range defined by the mean value ± 2 × standard deviation (see Fig. 4).

4. RESULTS

4.1. QUALITATIVE ANALYSIS OF VICKERS TESTS

Standard UO_2 fuels

For the unirradiated standard UO_2, the indentations had four cracks at the corners, in the axis of the impressions (Fig. 5a). According to the criterions described in section 3, several hundreds of indentations were considered as valid to determine both the Vickers hardness and the apparent fracture toughness. The measurements (impression diagonal and hardness, crack lengths, apparent fracture toughness) are given in Table 4, in Table 5 and in Table 6 respectively.

However, the crack patterns in the irradiated standard UO_2 fuels were quite different from the theoretical expected shape. At 15.6 GWd/tM, different cracks have formed at the corners but grain boundaries have also fractured around the impressions (Fig. 5b). Similar observations were noted for the indentations in the irradiated fuels at 32.8 and 38 GWd/tM. The grain boundaries of the irradiated standard UO_2 fuels are more susceptible to fracture than those of the unirradiated standard UO_2 fuels.

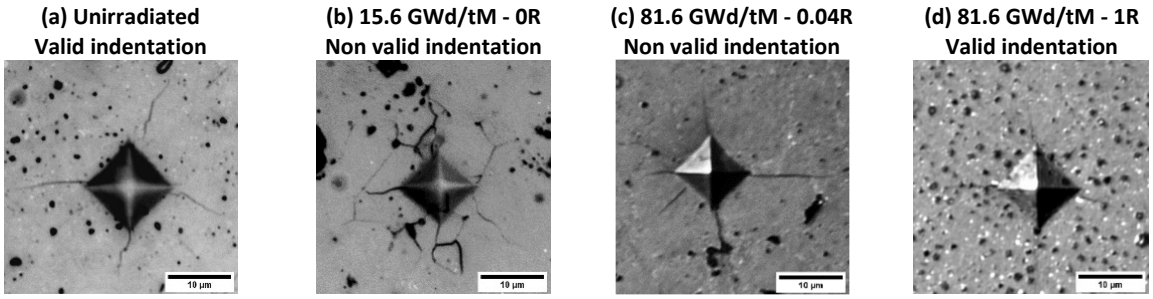

Fig. 5. Indentations in unirradiated and different irradiated standard UO_2 fuels (indentation load 0.735 N).

The high burnup standard UO_2 fuel at 81.6 GWd/tM (Fig. 5c) showed a similar behaviour, with cracked grain boundaries mainly observed between 0.5 and 0.75 R. In the centre of the pellet, the grain boundaries were slightly less cracked as shown in Fig. 5c at 0.04 R. At 0.04 R, bubbles observed around the impressions might have stopped the cracks. At 1 R (rim zone), even if, in the HBS, the size of the impression (2a) was much larger than the size of the submicron grains (Fig. 5d), cracks formed in the corners of the impressions, with a quite expected shape.

The behaviour of the other high burnup standard UO_2 fuel at 72.2 GWd/tM was very similar to that of the standard UO_2 - 81.6 GWd/tM fuel.

For the standard UO_2 out of the restructured zones, defined hereafter “non-restructured” fuels, as the dimensions of the impressions (*2a*) are close to those of the grains, each indent reached a grain boundary that fractured thus modifying the expected crack pattern. In this case, no valid indentation was found to measure valid crack lengths. Therefore, the fracture toughness of the non-restructured irradiated standard UO_2 was not calculated. For the irradiated standard UO_2, measurements of the fracture toughness were only performed on the periphery of the pellet where the fuel is partially (pre-rim) or totally restructured (rim). The measurements are given in Table 5 and in Table 6.

In order to quantify the embrittlement of grain boundaries in irradiated standard UO_2 fuels, the total length of the cracks generated by Vickers indentation, including both cracks in the axis of the impressions and cracks of the grain boundaries, was measured in the centre (0 *R* to 0.4 *R*) and in the intermediate zone of each pellet (0.6 *R* to 0.7 *R*). The measured total crack length is plotted against the average burnup in Fig. 6. The length strongly increases between 0 and 15.6 GWd/tM. This increase is mainly due to the fracture of the grains boundaries. For the highest burnups (above 60 GWd/tM), the total crack length is lower with a further decrease between 72.2 and 81.6 GWd/tM.

In these very high burnup fuels, the crack lengths are also shorter in the centre of the pellets, where bubble precipitation occurs, than in the intermediate zone where bubble precipitation is low. Measurements performed on standard UO_2 were marked by red triangles.

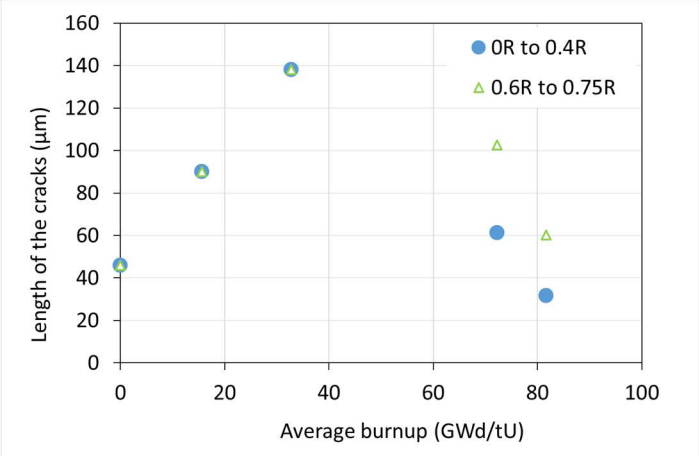

Fig. 6. Evolution of the length of the cracks, induced by Vickers indentation, in the centre (0R to 0.4R) and in the intermediate zone (0.6R to 0.75R) of standard UO_2, as a function of the average burnup (indentation load 0.735 N). The crack length is the sum of the length of straight cracks at the corners of the impressions and of the length of the cracked grain boundaries.

<u>Doped UO_2 fuels</u>

The indentations in the unirradiated and irradiated doped UO_2 with large grains of 60 µm were close to the expected theoretical shape with four cracks at the corners. Fig. 7 shows the evolution with the burnup of the indentations in the doped UO_2 up to 60.8 GWd/tM. Except in the rim (HBS) at 1R - 61 GWd/tM (Fig. 7d), the indentations in the different burnup fuels were quite similar (Fig. 7a, b, c). Many indentations were valid to calculate the Vickers hardness, the crack lengths and the Vickers fracture toughness. The measurements are respectively given in Table 4, in Table 5 and in Table 6. Measurements performed on doped UO_2 were symbolised by blue squares.

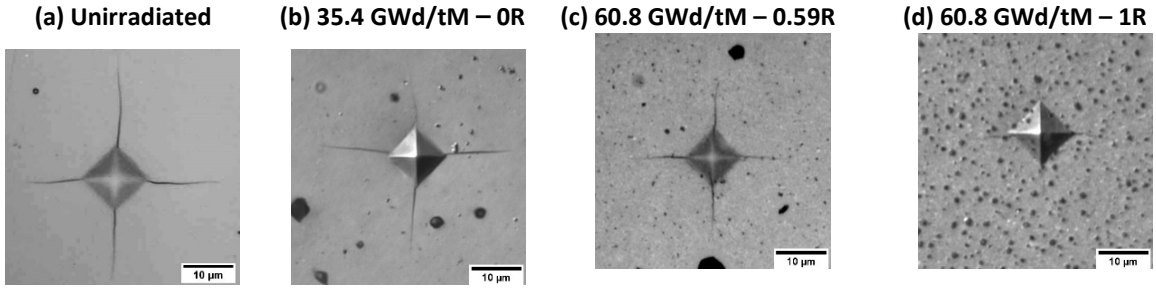

Fig. 7. Valid indentations in unirradiated and in irradiated doped UO_2 fuels with large grains (indentation load 0.735 N).

The grain boundaries were also brittle as shown in Fig. 8, but thanks to the large grains, it was possible to perform tests inside grains and to limit the influence of grain boundaries. However, this statement did not take into account what happened beneath the sample surface.

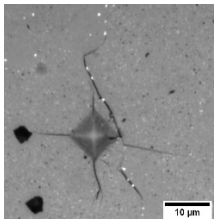

Fig. 8. Non-valid indentation in doped UO_2 with a burnup of 60.8 GWd/tM (indentation load 0.735 N).

4.2. VICKERS HARDNESS

The Vickers hardness of the unirradiated and irradiated standard and doped UO_2 fuels was calculated with the Eq.1, from the measurements of all valid impressions. The data are given in Table 4. In this Table 4, the local burnup is not the average burnup of the pellet given in Table 2, but the local burnup around the indent position, evaluated thanks to EPMA measurements of the *Nd* local concentration radial profiles. On each sample of unirradiated and irradiated fuels and according to the criterions described in the part 3, many valid impressions were available (see number of tests in Table 3).

The mean impressions diagonal for unirradiated fuels was between 14.3 and 14.6 µm for the standard fuel and between 13.4 and 13.6 µm for the doped fuel. For the irradiated and non-restructured fuels, outside the HBS, the size of the impressions was lower with a mean diagonal between 11.9 and 12.9 µm for the standard UO_2 and between 11.2 and 11.9 µm for the doped UO_2. In the HBS, both for standard and doped UO_2, the impressions were larger than in the non-restructured fuels with a mean diagonal between 13.2 and 14.2 µm.

Table 4: Impression diagonal and Vickers hardness of unirradiated and irradiated PWR UO_2 fuels (indentation load 0.735 N). For the high burnups fuels, the zone of the pellet is indicated (centre and intermediate zones: r/R<0.8 ; prerim ; rim). Average ± standard deviation

Fuel	Average burnup of the pellet (GWd/tM)	Local burnup (GWd/tM)	Number of valid indentations	Average impression diagonal *2a* (µm)	Vickers hardness (GPa)
Standard UO_2	0	0	20	14.5 *±0.3*	6.5 *±0.1*
Standard UO_2	0	0	54	14.3 *±0.4*	6.7 *±0.5*
Standard UO_2	0	0	32	14.6 *±0.3*	6.4 *±0.4*
Standard UO_2	15.6	15.4	48	12.4 *±0.4*	8.9 *±0.6*
Standard UO_2	32.8	31.8	45	12.2 *±0.5*	9.2 *±0.8*
Standard UO_2	38	36.6	27	12.6 *±0.5*	8.6 *±0.7*
Standard UO_2 – (r/R<0,8)	72.2	66	75	12.1 *±0.4*	9.3 *±0.6*
Standard UO_2 – Pre rim (r/R=0.880)	72.2	73.1	11	12.0 *±0.4*	9.5 *±0.6*
Standard UO_2 – Pre rim (r/R=0.960)	72.2	89.1	5	11.9 *±0.2*	9.6 *±0.4*
Standard UO_2 – Rim (r/R=0.988)	72.2	115	3	13.8 *±0*	7.2 *±0*
Standard UO_2 – Rim (r/R=0,990)	72.2	129	3	14.6 *±1.3*	6.4 *±1.0*
Standard UO_2 – Rim ((r/R=0,993)	72.2	142	3	14.8 *±0.6*	6.2 *±0.50*
Standard UO_2 (r/R<0,8)	81.6	74.2	55	12.3 *±0.4*	9.3 *±0.54*
Standard UO_2 – Pre rim (r/R=0.882)	81.6	92	5	12.4 *±0.3*	8.9 *±0.36*
Standard UO_2 – Pre rim (r/R=0.963)	81.6	103	5	12.9 *±0.2*	8.2 *±0.23*
Standard UO_2 – Rim (r/R=0.982)	81.6	116	6	12.7 *±0.3*	8.5 *±0.30*
Standard UO_2 – Rim (r/R=0.988)	81.6	124	5	13.7 *±0.4*	7.2 *±0.36*
Standard UO_2 – Rim (r/R=0,993)	81.6	138	4	14.2 *±0.3*	6.8 *±0.25*
Doped UO2	0	0	42	13.6 *±0.3*	7.8 *±0.3*
Doped UO2	0	0	20	13.4 *±0.3*	7.6 *±0.4*
Doped UO2	16.5	16.3	48	11.8 *±0.4*	9.8 *±0.6*
Doped UO2	35.4	34.1	69	11.8 *±0.4*	9.8 *±0.4*
Doped UO2 – (r/R<0,8)	60.8	57.1	52	11.4 *±0.4*	10.5 *±0.7*
Doped UO2 – Pre rim (r/R=0,855)	60.8	58.5	4	11.2 *±0.3*	10.9 *±0.6*
Doped UO2 – Pre rim (r/R=0,933)	60.8	62.2	3	11.9 *±0.3*	9.6 *±0.4*
Doped UO2 – Rim (r/R=0,980)	60.8	88.3	4	13.6 *±0*	7.4 *±0*
Doped UO2 – Rim (r/R=0,984)	60.8	96.2	3	13.7 *±0*	7.3 *±0*
Doped UO2 – Rim (r/R=0,986)	60.8	104.6	2	13.7 *±0.1*	7.2 *±0.2*
Doped UO2 – Rim (r/R=0,990)	60.8	116.2	5	13.9 *±0.2*	7.1 *±0.2*

Examples of the radial evolution of the Vickers hardness of both the irradiated standard fuel at a burnup of 81.6 GWd/tM and of irradiated doped fuel at a burnup of 60.8 GWd/tM are given respectively in Fig. 9 and in Fig. 10. The limit of the precipitation zone in the centre of the pellet is

determined using the EPMA Xe radial profile. The pre-rim and rim limits are determined by OM. The evolution of high burnup fuels is similar, as illustrated in Fig. 9 and Fig. 10. The Vickers hardness is nearly constant from the centre to 0.8 R. It decreases on the periphery of the pellet, in pre-rim and in the rim (HBS), where the local burnup (Fig. 9) and the porosity are larger (Fig. 10). In the pre-rim, the fuel is partially restructured into HBS.

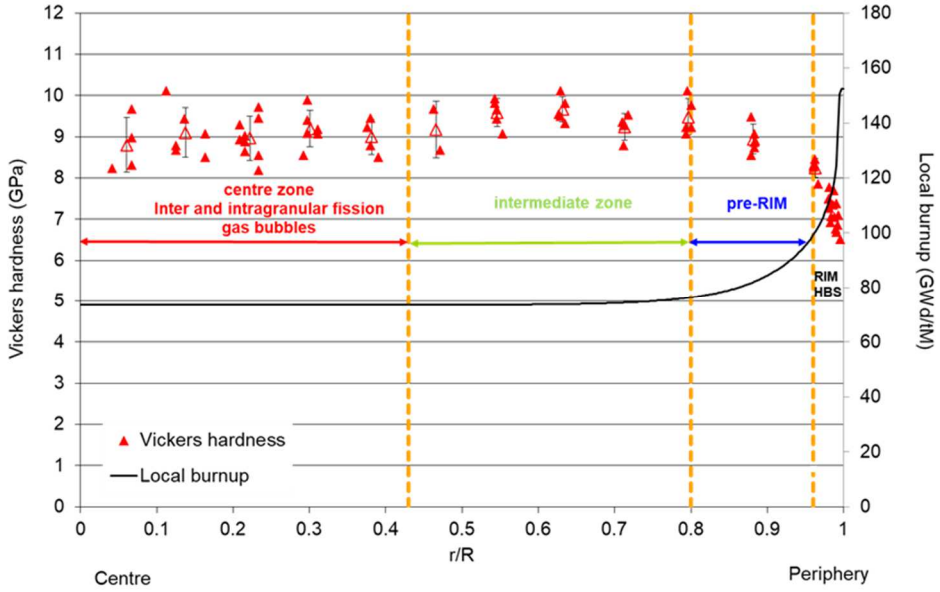

Fig. 9. Vickers hardness (indentation load 0.735 N) and local burnup of the irradiated standard UO_2 - 81.6 GWd/tM as a function of the radial position. The local burnup was deduced from the neodymium content, measured by EPMA. The single hardness values are indicated by solid triangles and the average value of hardness at 12 radial positons is indicated by empty triangles. In the pre-rim zone, the fuel is partially in the HBS and in the rim zone, the fuel is totally in the HBS.

In more details, little differences exist between the centre and the intermediate zones: Vickers hardness is lower in the centre where fission gas bubbles precipitated. The evolution of the Vickers hardness with the burnup is discussed in section 4.4.1.

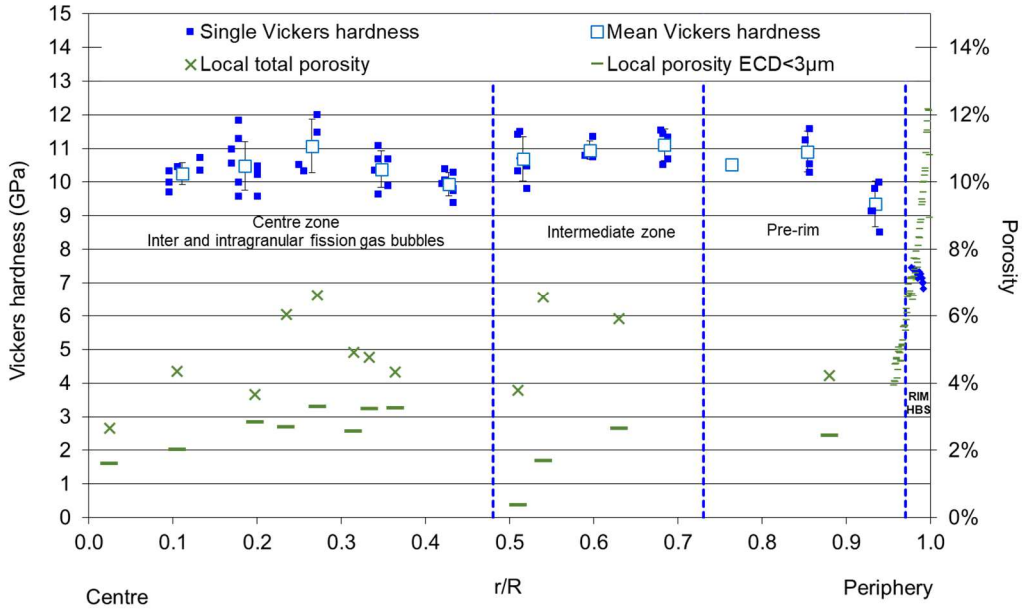

Fig. 10: Vickers hardness (indentation load 0.735 N) and local porosity (total and ECD<3 µm) of the irradiated doped UO_2 – 60.8 GWd/tM as a function of the radial position. The local porosity was determined by SEM images analysis. The single hardness values are indicated by blue solid squares and the average value of hardness at 11 radial positons is indicated by blue empty squares. Inter-granular and intra-granular fission gas bubbles are precipitated in the centre zone. The

intermediate zone with less bubbles. In the pre-rim zone, the fuel is partially in the HBS and in the rim zone, the fuel is totally in the HBS.

4.3. VICKERS INDENTATION FRACTURE TOUGHNESS

The measurements of the crack lengths *c* and *l* (as defined in Fig. 4) for valid imprints are given in Table 5.

Table 5: Vickers crack lengths c and l of unirradiated and irradiated PWR UO_2 fuels (indentation load 0.735 N). For the high burnups fuels, the zone of the pellet is indicated (centre and intermediate zones: r/R<0.8 ; prerim ; rim).

Fuel	Average burnup of the pellet (GWd/tM)	Local burnup (GWd/tM)	Number of valid indentations	Average crack length *c* (µm)	Average crack length *l* (µm)
Standard UO_2	0	0	42	16.3 *±1.4*	9.2 *±1.4*
Standard UO_2	0	0	32	15.4 *±1.4*	8.1 *±1.4*
Standard UO_2	0	0	10	16.0 *±1.4*	8.8 ±1.4
Standard UO_2 – Pre rim (r/R=0.882)	81.6	82.0	3	9.3 *±0.6*	3.1 *±0.6*
Standard UO_2 – Rim (r/R=0.974)	81.6	110.8	9	10.1 *±1.1*	3.4 *±1.0*
Standard UO_2 – Rim (r/R=0.992)	81.6	132.6	5	9.4 *±1.3*	2.3 *±1.3*
Doped UO_2	0	0	20	22.0 *±2.2*	15.4 *±2.2*
Doped UO_2	0	0	42	21.2 *±2.3*	14.5 *±2.3*
Doped UO_2	16.5	16.3	4	16.4 *±1.4*	10.5 *±1.4*
Doped UO_2	35.4	34.1	44	17.1 *±2*	11.2 *±2*
Doped UO_2 – (r/R<0.8)	60.8	57.1	35	16.9 *±1.4*	11.1 *±1.4*
Doped UO_2 – Pre rim (r/R=0.894)	60.8	60.4	4	14.3 *±1.6*	8.6 *±1.6*
Doped UO_2 – Rim (r/R=0.982)	60.8	91.7	7	11.4 *±0.5*	4.6 *±0.5*
Doped UO_2 – Rim (r/R=0.989)	60.8	112.9	7	10.3 *±0.8*	3.4 *±0.7*

As already mentioned in sections 3 and 4.1, a limited number of indentations were considered as valid to measure the fracture toughness in irradiated fuels. No valid indentation was obtained for the standard grain UO_2 irradiated fuels apart from the pre-rim and the rim zone where the fuel is partially or totally in the HBS. For the unirradiated fuels, the cracks were longer in the doped UO_2 than in the standard UO_2 (see Fig. 11). In the central and intermediate zones of the pellet, the average length of the cracks for the doped UO_2 decreased quickly during the first cycle of irradiation but then remained constant with the local burnup up to 60 GWd/tM. A decrease was then observed when the fuel restructured into HBS on the pre-rim and rim zones. The length of the cracks in the HBS of standard UO_2 and doped UO_2 was similar.

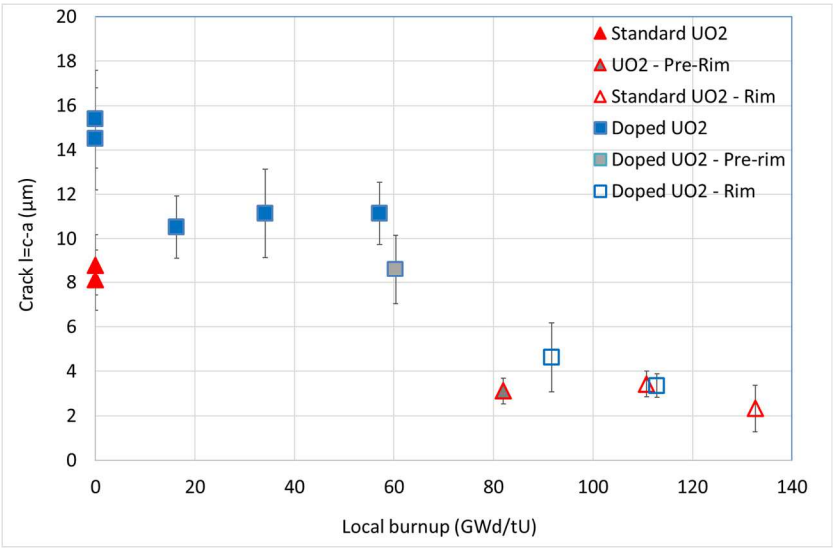

Fig. 11. Crack length l in standard UO_2 and doped UO_2 as a function of the local burnup (indentation load

0.735 N). For the high burnups fuels >50 GWd/tM, the prerim and rim zones of the pellet are presented in light gray and with open signs respectively; otherwise, the fuels come from the centre and the intermediate zones (r/R<0.8).

To calculate the fracture toughness, the porosity is given in Table 2. In HBS, the authors determined the local porosity at the local position of each HBS indent.

The fracture toughness of the fuels calculated with the Niihara equation (Table 3 – Eq.2) are given in Table 6. In the HBS of high burnup samples for both standard and doped UO_2, indent diagonals were more than ten times larger than the grain size. The cracks were well-formed in the axis of the impressions and fracture toughness could be measured. Small changes in the crack (interaction with grain boundaries of the HBS) are shown in Fig. 12.

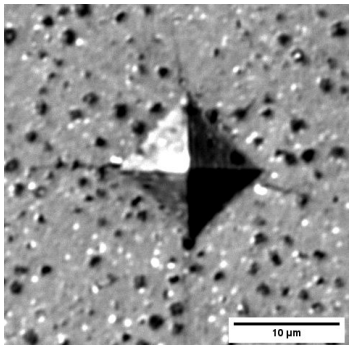

Fig. 12. Impression in the HBS of the rim (indentation load 0.735 N)

In Fig. 13, *c/a* ratio for the different fuels is plotted as a function of the local burnup. The ratio is higher than 2 for non-restructured fuels, but in the HBS, the *c/a* is lower than 2. In the pre-rim where the fuel is partially in the HBS, *c/a* is higher than 2 for the doped UO_2 but lower than 2 for the Standard UO_2. As already mentioned, a transition from Palmqvist (c/a < 2) to Half penny mode (*c/a* > 2) is usually noted in literature [25][28]. In the HBS, *c/a* is lower than 2 therefore fracture toughness calculated with equations for Halfpenny mode are not suited. Equations for Palmqvist mode should then be preferred.

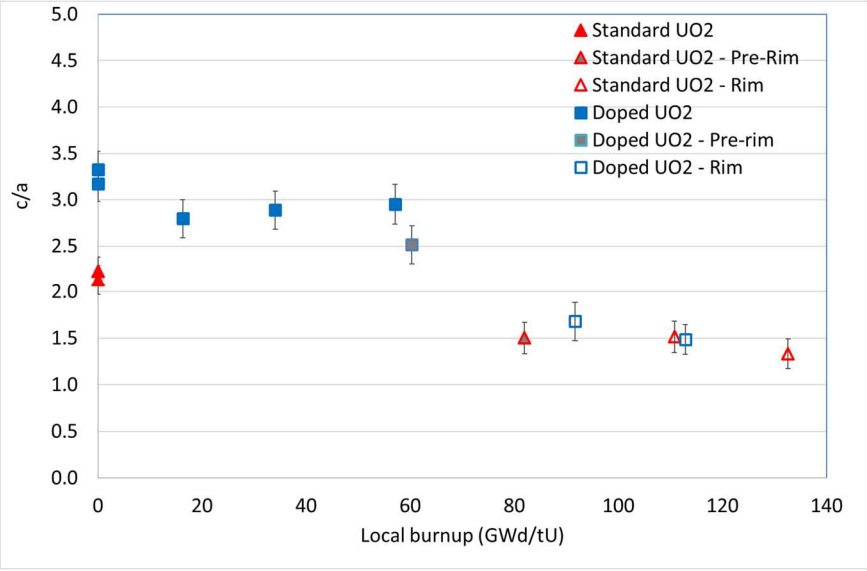

Fig. 13. Ratio c/a as a function of the local burnup for the standard UO_2 and the doped UO_2 (indentation load 0.735 N). For the high burnups fuels >50 GWd/tM, the prerim and rim zones of the pellet are indicated in the legend ; otherwise, the fuels come from the centre and the intermediate zones (r/R<0.8).

The different Palmqvist equations proposed in the literature could give quite variable results. The results obtained with different equations are shown in Table 6. The measurements with Casellas equation are very close to the results with the Niihara equation in Palmqvist mode. Laugier equation

leads to high values of apparent fracture toughness in the HBS. In the HBS, the Vickers fracture toughness was calculated with the Niihara equations in Palmqvist mode (Table 3 – Eq.4). The values were between 1.38 and 2.83 MPa.m$^{0.5}$ in Half penny mode and between 1.21 to 2.04 MPa.m$^{0.5}$ in Palmqvist mode (Table 6). Finally, the assumed crack geometry is not found to significantly affect the results.

Table 6: Fracture toughness (MPa.m$^{0.5}$) of unirradiated and irradiated PWR UO_2 fuels, calculated with several equations (indentation load 0.735 N). The equations are given in Table 3. For the high burnups, the zone of the pellet is indicated (centre and intermediate zones: r/R<0.8 ; prerim ; rim).

Fuel	Local burnup (GWd/tM)	Anstis Eq. n°1	Niihara Eq. n°2	Matzke Eq. n°5	Niihara Eq. n°4	Laugier Eq. n°3	Casellas Eq. n°6
Standard UO_2	0	0.92	1.37	1.18	1.13	1.32	1.44
Standard UO_2	0	1.04	1.54	1.33	1.21	1.62	1.63
Standard UO_2	0	0.96	1.42	1.23	1.15	1.42	1.50
Standard UO_2 – Pre rim (r/R=0.882)	82.0	1.76	2.71	2.34	1.90	3.77	2.73
Standard UO_2 – Rim (r/R=0.974)	110.8	1.66	2.53	2.18	1.77	3.59	2.58
Standard UO_2 – Rim (r/R=0.992)	132.6	1.84	2.81	2.42	2.02	4.96	2.87
Doped UO_2	0	0.55	0.82	0.71	0.88	0.56	0.85
Doped UO_2	0	0.60	0.90	0.77	0.93	0.65	0.93
Doped UO_2	16.3	0.76	1.17	1.01	1.11	0.87	1.19
Doped UO_2	34.1	0.73	1.13	0.97	1.08	0.82	1.14
Doped UO_2 (r/R<0,8)	57.1	0.70	1.09	0.94	1.06	0.75	1.09
Doped UO_2 – Pre rim (r/R=0.894)	60.4	0.88	1.38	1.19	1.20	1.07	1.37
Doped UO_2 – Rim (r/R=0.982)	91.7	1.45	2.19	1.89	1.56	2.78	2.26
Doped UO_2 – Rim (r/R=0.989)	112.9	1.68	2.54	2.19	1.78	3.79	2.61

4.4. DISCUSSION

4.4.1. Effects of irradiation on Vickers hardness

Vickers hardness is plotted as a function of the local burnup for all tested samples in Fig. 14. For both fuels, standard and doped, Vickers hardness increases clearly during the first cycle of irradiation and decreases when the fuel restructured into HBS. The Vickers hardness is about 6.5 GPa for the unirradiated standard UO_2 and 7.7 GPa for the unirradiated doped UO_2. It is about 9 GPa for the non-restructured standard irradiated UO_2 and 10 GPa for the non-restructured irradiated doped UO_2. Despite the larger grain size of the doped UO_2, the non-restructured doped UO_2 is always harder than the non-restructured standard UO_2 at different local burnups.

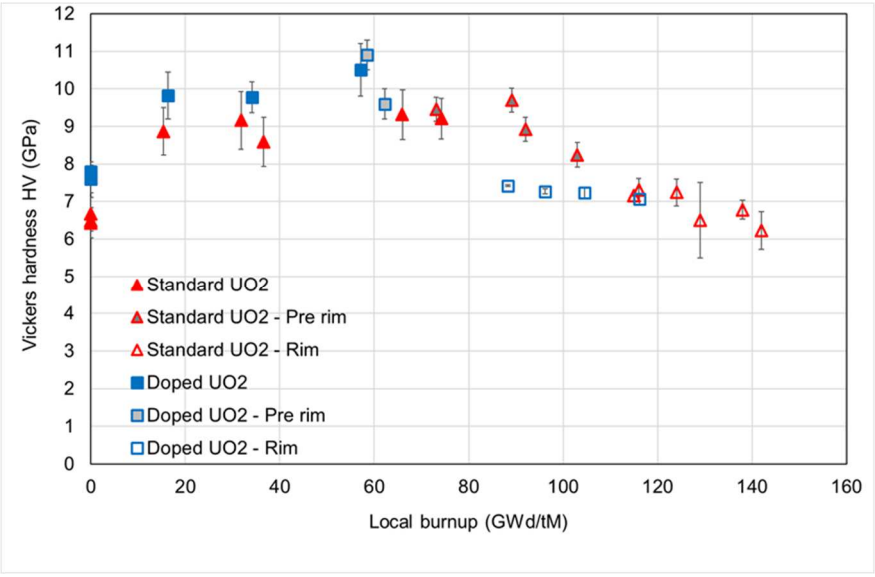

Fig. 14. Evolution of the Vickers hardness of UO_2 fuels with the local burnup of the pellet (indentation load 0.735N). For

the high burnups fuels >50 GWd/tM, the prerim and rim zones of the pellet are presented in light gray and open sign respectively; otherwise, the fuels come from the centre and the intermediate zones (r/R<0.8).

Hardening was also measured by McDonald *et al*. on a fresh large grain UO_2 fuel doped with TiO_2 [33]. No clear explanation to these higher hardness measurements in Cr doped UO_2 are brought here.

The hardening fuel was not due to the porosity rate because some doped and un-doped UO_2 fuels had the same porosity rate. According to the Hall-Petch effect [35], the increase in grain size should have led to lower fuel harnesses. Similarly, for the samples in this study, the hardening could be due to the chromium doping in solid solution. However, one could then expect that the effect of this doping would mingle with the effect of fission product, build-up with quickly higher fission product content than Cr content. Therefore, the doping might not be the direct reason for this higher hardness.

For both restructured irradiated standard and doped UO_2, the Vickers hardness decreases to reach 6.2 GPa at a local burnup of 140 GWd/tM. In the HBS, the hardness of the doped and standard UO_2 are similar for similar local burnups.

Xiao *et al.* [34] calculated a Vickers hardness of 6.7 ± 0.2 GPa for an unirradiated UO_2 at a lower applied load of 0.3 N. The porosity fraction was 2.4% and the grains size was between 20 and 30 µm. In this work, the Vickers hardness of the standard UO_2, about 6.5 GPa, is in good agreement with Xiao *et al*.

Spino *et al.* [32] proposed also the evolution of the Vickers hardness with the average burnup for LWR Standard UO_2 fuels with a grain size of 7-10 µm and at a similar applied load of 0.5 N. In this case, the Vickers hardness was measured in the central part of the pellet with $r/R < 0.8$ for a transverse section and $r/R < 0.5$ for a longitudinal section. The values of Spino *et al.* are compared to our results in the non-restructured fuel, in Fig. 15.

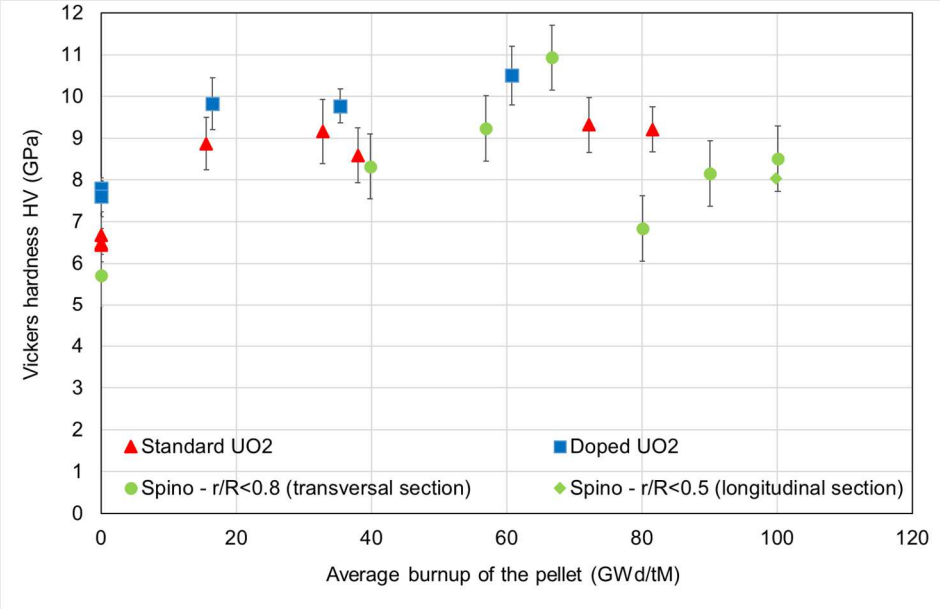

Fig. 15. Evolution of the Vickers hardness of UO_2 fuels with the average burnup of the pellet in the non-restructured fuel. For the high burnups fuels >50 GWd/tM, the fuels (red triangles for the

Standard UO_2 and blue squares for the doped UO_2 come from the centre and the intermediate zones (r/R<0.8).

Data are found to be in a similar range of values. However, some differences are noted with our work.

First, Spino *et al.* [32] found a decrease in the Vickers hardness in the centre and the intermediate zones of the pellet between 70 and 80 GWd/tM. This decrease was not observed up to 81.6 GWd/tM in our study, as shown in the radial profiles (Fig. 16).

A second difference deals with the evolution of the Vickers hardness with the burnup. Spino *et al.* proposed a linear increase of the hardness with the burnup, but had made no measurement at low burnups, i.e. one irradiation cycle fuels. With additional values at lower burnups (15 to 20 GWd/tM), we rather propose a quick increase of hardness during the first cycle of irradiation followed by a limited increase with the irradiation level (outside the HBS). This hardening is due to irradiation defects such as dislocations and fission products [32].

In restructured fuels, Spino *et al.* [32] observed a similar decrease of hardness as noted in this work. This evolution is due the local microstructure changes, including the porosity fraction increase up to 15-17 % and the grain size restructuration [10][32]. The effect of grain size restructuration is expected to increase hardness, according to the Hall-Petch effect [35]. Gong *et al*. [40] studied unirradiated nanocrystalline and microcrystalline UO_2 samples with a porosity of about 3.5% and 3.7% respectively. They indeed measured a larger hardness in nanocrystalline microstructure (10.9 ±0.7 GPa) as compared to microcrystalline microstructure (6.8 ±0.4 GPa). It appears therefore that the decrease in hardness of HBS is mainly explained by their higher porosity. One can note that the slope of the decrease of hardness with porosity is smaller for HBS than for unirradiated fuels. The influence of grain size (smaller in HBS) could partly explain this difference. Spino *et al*. [32] also mentioned the difference in pore shapes between HBS and non-irradiated fuels: sintered fresh fuels were described by solid spheres with small inter-granular pores, whereas HBS fuels were described by spherical pores separated by smaller solid walls. The difference in behaviour between HBS and non-irradiated fuels could also be related to the presence of fission products in irradiated HBS fuels or to the effect of alpha decay during storage (see part 4.4.2).

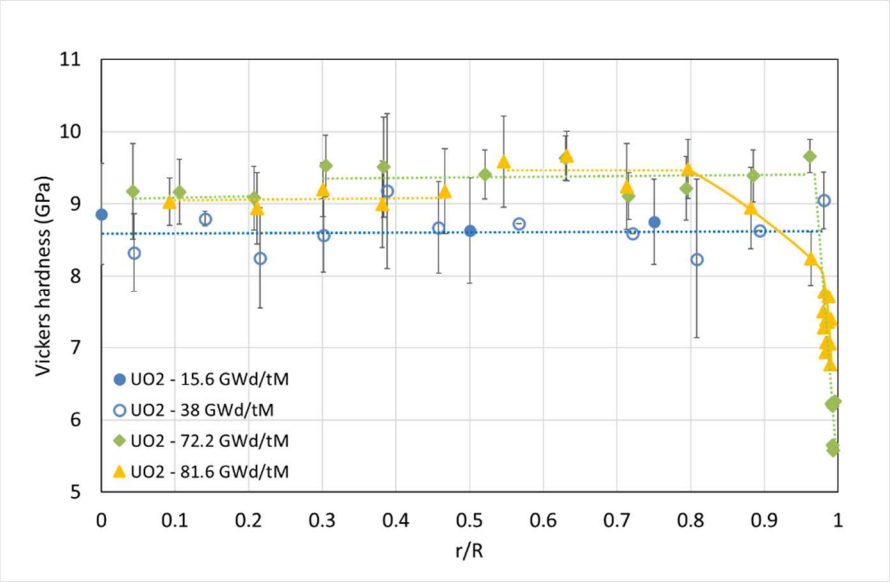

Fig. 16. Evolution of the Vickers hardness profiles of standard UO_2 fuels with the average burnup of the pellet (indentation load 0.735 N).

4.4.2. Effect of storage on Vickers hardness

Mechanical properties evolution of materials is directly linked to the evolution of defects created by irradiation [41]. In spent UO_2 fuels, after decay of the beta decaying short lived fission products, significant quantity of alpha emitters created with irradiation in reactor can also lead to irradiation damage in the spent fuel by self alpha radiation thus possibly modifying mechanical properties of fuels during storage time. Wiss *et al*.[42] showed that the magnitude of the evolution of Vickers hardness in alpha-damaged Pu doped unirradiated UO_2 was comparable to that measured in this study (Fig. 17). The evolution in Pu doped UO_2 was indeed about 7 GPa untill an alpha-dose of 1×10^{16} alpha decays.g^{-1} to 9 GPa after an alpha-dose of 2×10^{17} alpha decays.g^{-1}.
The UO_2 fuel alpha damages during storage time depend on alpha emitter build-up, related to the initial ^{235}U enrichment and increasing with burnup, and on storage time. In this paper, different irradiated UO_2 fuels were studied with various burnups and storage times. Moreover, high burnup fuels exhibit a radial evolution of burnup and alpha emitter build-up with higher values in the periphery of the fuels, and particularly on the rim of pellets.
Alpha decays during storage were calculated along the pellet radius of each studied fuel sample, using the Prodhel model [43] used in the Alcyone fuel performance code [21] considering a local isotopic composition and irradiation linear powers.
In the r/R <0.8 zone, alpha-doses cumulated during fuels storage were between 6.9×10^{15} and 2.7×10^{17} alpha decays g^{-1}. Vickers hardness of studied spent UO_2 were compared to the results obtained by Wiss *et al*. in Fig. 17. Hardness measurements of irradiated fuels were in the range where Wiss *et al*. measured a hardness evolution with alpha decays damages. However, the hardness of irradiated fuels was already saturated, around 9 GPa, by irradiation defects, as it can be noted with the measurements at low burnup and short storage time, with alpha decay doses in the low region of the transition zone determined by Wiss *et al*. on Pu doped unirradiated UO_2. Moreover, the UO_2 – 31 GWd/tM fuel with a short storage time (~2 years – 2.9×10^{16} alpha decays g^{-1}) and the UO_2 – 38 GWd/tM fuel with a long storage time (~18 years - 2×10^{17} alpha decays g^{-1}) showed a similar hardness. The considered effect of storage does not seem further increase the Vickers hardness after irradiation in reactor.

In the centre of the pellet where the temperature is higher than in the periphery, defects annealing could occur, followed by hardening due to the storage damages that would erase the annealing effect. In this case, the hardness profiles of irradiated fuels with short storage should show a hardness decrease. As no significant decrease at the centre of the pellet where the temperature is higher than in the periphery (Fig. 16) was noted on hardness profiles (Fig. 16), neither at low burnup nor at short storage time, no defects annealing is observed in the studied PWR UO_2 fuels.

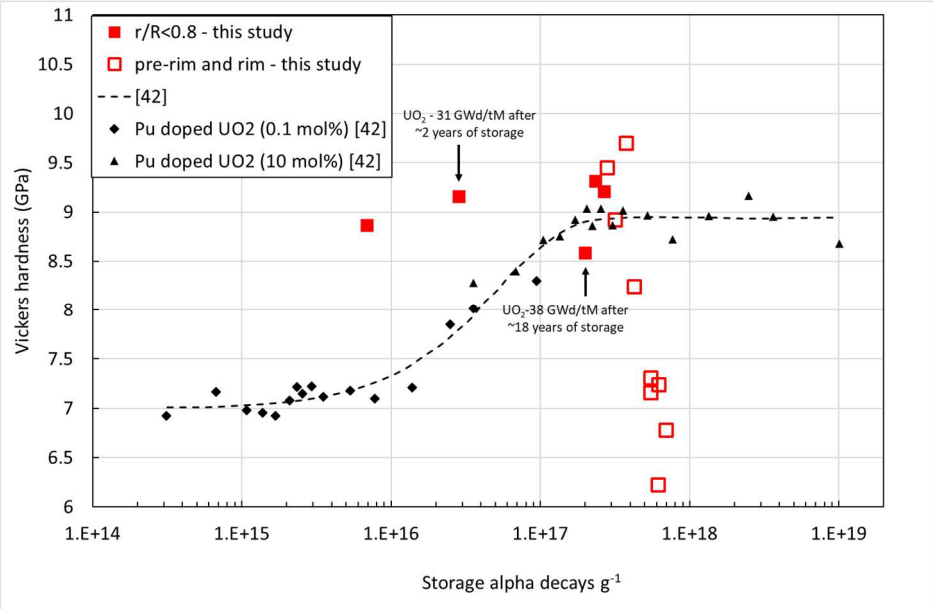

Fig. 17. Vickers hardness as a function of alpha decay densities. In this study, the UO_2 samples were irradiated in a reactor at different burnups. The alpha decays were calculated during storage time with the Prodhel model [43]. The [42], unirradiated Pu doped UO_2 samples accumulated alpha dose during their storage

In the pre-rim and the rim zones, the alpha-doses cumulated during the storage of studied fuels ranged between 1.6×10^{17} and 7×10^{17} alpha decays.g^{-1}, i.e. in the range of values for which Wiss *et al*. measured a hardness saturation around 9 GPa due to alpha decay damages. The saturation of hardening was not measured in HBS areas of these irradiated fuels, on contrary a significant softening was found. This decrease in hardness can be explained by the build-up of porosity in the HBS formation process. However, by comparing HBS hardness with that of porous fresh fuels with different porosity fractions, Spino et al [32] showed that the expected decrease in hardness should be stronger in irradiated HBS fuels. They attributed this difference to pore shape differences between porous fresh fuels and HBS (cf 4.4.1). It could, actually, also be related to the presence and the local distribution of fission products in irradiated HBS fuels. Another reason for this difference might be also a hardening effect of alpha decays during storage. Dedicated Vickers hardness measurements on high burnup fuels with very short storage times would be necessary to further support this hypothesis.

4.4.3.Comparison of Vickers fracture toughness with literature

Kutty *et al.* [9] determined the indentation fracture toughness on unirradiated standard UO_2 with Vickers indentation at a load of 294 N. For a porosity of 5%, the average fracture toughness obtained with the Anstis equation (Table 3 – Eq.1) was 0.9 MPa.$m^{0.5}$. More recently, Xiao *et al.* [34] also calculated the unirradiated standard UO_2 (2.4% porosity) Vickers fracture toughness using the Anstis equation with a lower load of 0.3 N. The grains size was between 20 and 30 µm. The resulting fracture toughness of UO_2 was 1.12 ± 0.02 MPa.$m^{0.5}$.

In this paper, the Vickers fracture toughness measured on unirradiated standard UO_2 with the Anstis equation was between 0.92 and 1.11 MPa.$m^{0.5}$ (Table 6). These results are in good agreement with Kutty *et al.* and Xiao *et al* and do not seem not to be largely impacted by the difference of testing load.

Although in our work Vickers indents were considered as non-valid for fracture toughness measurements in irradiated standard UO_2, Spino *et al.* [32] managed to determine a radial profile of the fracture toughness on an irradiated UO_2 with a grain size between 7-10 µm, for a burnup of

0.3 GWd/tM and a load of 0.5 N. For $r/R < 0.8$, the fracture toughness calculated with Matzke equation was similar to our measures on unirradiated standard fuels, around 1.25 ± 0.5 MPa.m$^{0.5}$.

4.4.4. Effects of irradiation on the fracture toughness

Fig. 18 plots the Vickers fracture toughness of the doped UO_2 versus the local burnup. It shows that the Vickers fracture toughness increases during the first irradiation cycle and is subsequently constant with the burnup up to 60 GWd/tM in the central and intermediate zones.

The equations for Vickers fracture toughness (Table 3) are all function of the ratio of the Young's modulus over the hardness (*E/H*) and of the crack length *c*. With the irradiation, the *E/H* ratio doesn't change significantly because the Young's modulus calculated from porosity values decreases and the hardness increases (Fig. 15). As the mean length *c* of the cracks decreases (Table 5), the increase in Vickers fracture toughness of the doped UO_2 fuel with the burnup is mainly explained by the decrease of the length *c*. Furthermore, Kutty *et al*. [9] showed that the crack length *c* decreased when the porosity fraction increased in nuclear fuels. The cracks length decrease with irradiation is probably linked to the presence of bubbles and defects such as fission products precipitates formed during irradiation and the associated residual stresses generated [1].

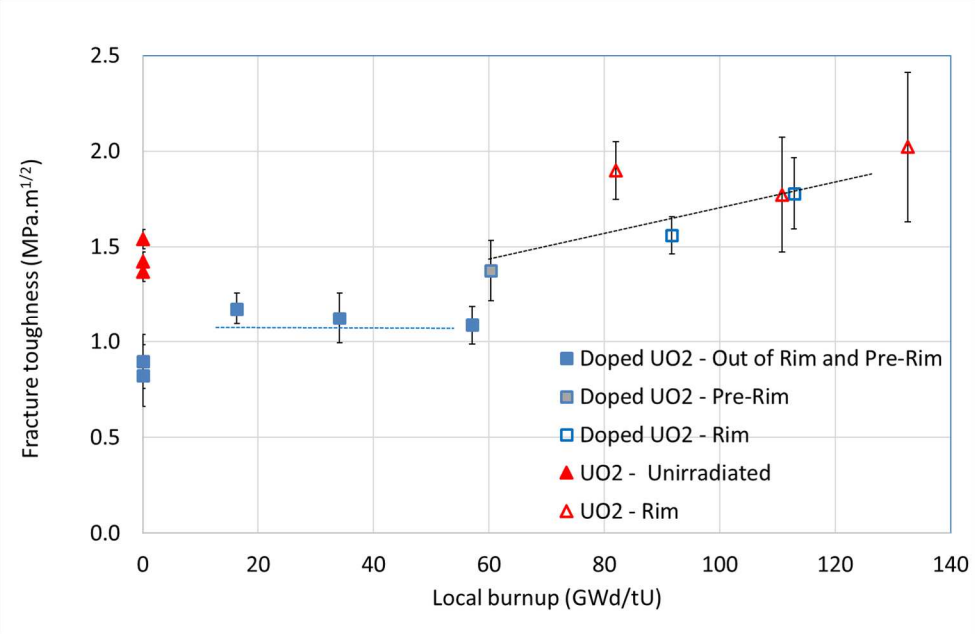

Fig. 18. Fracture toughness of standard and doped UO_2 as a function of the local burnup (indentation load 0.735 N). For the non-restructured fuel (< 60 GWd/tM), tests were realized inside single grains only on doped UO_2. The fracture toughness was calculated with the Niihara equation in Half penny mode (Table 3 – Eq.2). For the HBS UO_2 and HBS doped UO_2 (60 GWd/tM ≤), the fracture toughness was calculated with the Niihara equation in Palmqvist mode (Table 3 – Eq.4).

Fracture toughness measurements were made on the unirradiated standard UO_2 where indentations cracks are always longer than grains and therefore crossed grain boundaries. The unirradiated standard UO_2 had a fracture toughness between 1.37 ± 0.14 and 1.54 ± 0.14 MPa.m$^{0.5}$ against 0.82 ± 0.14 to 0.9 ± 0.16 MPa.m$^{0.5}$, for the unirradiated doped UO_2. The higher fracture toughness of the unirradiated standard UO_2 was probably due to the effect of the grain boundaries that deviated the propagation of the crack, acting as a crack shield. Tests realized on single crystals and polycrystalline samples of cubic zirconia also showed that the grain boundaries seemed to increase the apparent indentation fracture toughness [12].

In HBS, the apparent fracture toughness values were higher than in the non-restructured irradiated fuels (Fig. 18). As in HBS, the Young's modulus and the hardness decreased as compared to the non-restructured fuel, the ratio *E/H* was similar for both zones. The high fracture toughness in the HBS is mainly due to the propagation of short cracks around large impressions. Gong *et al*. [40] also showed a similar increase in fracture toughness determined by indentation from microcrystalline to nanocrystalline microstructures. They showed that for nanocrystalline UO_2, the fractures surface showed typical inter-granular fracture with cracking propagation along the grain boundaries. Cracks deflected on the weak grain boundaries, also already noted in [32][36]. As suggested by Terrani *et al.* [36], the higher apparent fracture toughness could be explained by the crack deflection at grain boundaries, requiring a higher energy than in the case of a straight crack. Moreover, the equations used for the determination of fracture toughness may not be appropriate for the HBS with an important porosity (6 to 15%). Densification under the indenter may reduce the residual tensile stress field and the calculated fracture toughness may then be overestimated. In the HBS, local micro-cantilever tests are an option to estimate the local fracture toughness but these tests are delicate to run due to the large fraction of bubbles and defects. The possible influence of defects on the fracture could be modelled as recently illustrated by Doitrand *et al.* [39].

4.4.5. Comparison of fracture toughness by Vickers indentation and by micro-bending tests

Henry *et al.* performed micro-cantilever bending tests on an unirradiated standard UO_2 fuel and also on an irradiated standard UO_2 fuels at a burnup of about 35 GWd/tM, to determine the local fracture properties [13][14]. The tests were realized inside grains. The fracture toughness of the unirradiated and irradiated UO_2 fuels were quite similar for both materials and varied from 1.24 to 2.28 $MPa.m^{0.5}$ with an average value of 1.68 ± 0.31 $MPa.m^{0.5}$, i.e. in the same range of magnitude as the values for indentation tests. However, unlike Vickers results, these tests inside grains did not show any evolution of the fracture toughness between unirradiated and irradiated standard UO_2 fuels.
Such local tests differ from indentation tests as performed in this study. Firstly, the beam fabrication may affect the results with a relaxation of residual stresses in the irradiated fuels or with the ion implantation, already known to influence the toughness measurement as noted on some materials [37] but not on others [38]. Moreover, the fuel volume that interacts with the cracks is smaller for micro-bending tests than for Vickers tests.
On overall, these techniques appear as complementary and needed to be further compared, as they give access to critical data for modelling.

5. CONCLUSIONS

Hundreds of Vickers indentations were realized at room temperature and with a load of 0.735 N on UO_2 fuels with standard (~10 µm) and large (~60 µm) grains, irradiated up to a high burnup of 81.6 GWd/tM. For the high burnup samples, the fuels were restructured in the HBS on the periphery of the pellet, with small grains (< 1 µm) and many fission gas bubbles.

Vickers hardness of both standard UO_2 and doped UO_2 increased quickly during the first cycle of irradiation and then slightly increased up to a burnup of 81.6 GWd/tM. Finally, it decreased when the fuel restructured in the HBS. The comparison with data in literature shows that at high burnups, differences in fuel fabrication or in irradiation conditions leading to changes in gas bubble or other fission product precipitations, may affect Vickers hardness. In HBS, the hardness decrease is probably mainly due to the larger porosity.

Since measurements were performed on spent irradiated fuels after some storage time, the possible effect of alpha decay damages cumulated during the storage time was evaluated using results established on fresh fuels doped with alpha emitters [42]. It was compared to the effect of irradiation in reactor. The magnitude of each separate effect is similar. However, in irradiated fuels, the hardness in reactor saturated quickly with the irradiation defects created and masked any potential effect of storage on the Vickers indentation measurements.

Vickers tests showed the presence of fractured grain boundaries around the impressions in the non-restructured irradiated UO_2 fuels but not in the unirradiated fuels. Therefore, in order to obtain valid measurements of fracture toughness on irradiated fuels, the indentations have to remain inside the grains. Consequently, fracture toughness measurements on irradiated fuels were only performed on doped UO_2 fuels with large grains, indentation impressions having a size equivalent to the grain size of the standard UO_2 fuel. In the HBS, even if the grain boundaries were weak, the cracks were well formed in the axis of the impressions' corners.
The evolution of the Vickers fracture toughness with the local burnup in the doped UO_2 showed a first rapid increase during the first cycle of irradiation, followed by a plateau for the irradiated non-restructured fuel. This increase was mainly linked to the decrease of the crack length, attributed to the interactions of the cracks with defects such as bubbles.
The fracture toughness of the unirradiated standard UO_2 was found to be higher than in unirradiated doped UO_2. For the standard UO_2 fuel, the average grain size is of the order of the indent size. Therefore, the indentations in standard UO_2 fuels always intercepted grain boundaries, on contrary to the doped UO_2 fuel. The difference in the fracture toughness results could be an effect of the grain boundaries acting as barriers and reinforcing the crack propagation resistance. To avoid the grain boundaries influence and to compare the properties of the unirradiated and the irradiated standard UO_2 fuels in the bulk, a decrease of the impressions size is required.
In the HBS, for the highest burnup samples and on the periphery of the pellet, short cracks followed grain boundaries of small grains, leading to an increased fracture toughness. The calculated toughness was similar for both standard and doped UO_2. The increase of HBS fracture toughness could be mainly due to grain size restructuration, rather than larger porosity. However, because of the high porosity in this zone, the use of the literature equations to calculate the apparent fracture toughness was questioned.

6. ACKNOWLEDGEMENTS

All the fuels in this paper were studied in the framework of a collaboration with EDF and FRAMATOME.
The authors would also like to thank J. Dailly, C. Blay, T. Charret who performed indentation tests of irradiated fuels during their training, V. Basini and JC. Ménard who realized indentation tests on some of the unirradiated fuels and most of the people working in the CEA LECA-STAR hot cell facility at Cadarache.

7. REFERENCES

[1] D. Baron, L. Hallstadius, K. Kulacsy, R. Largenton, J. Noirot, "Fuel Performance of Light Water Reactors (Uranium Oxide and MOX)", Volume Materials Science and Materials Engineering, Volume 2, 2020, Pages 35-71
[2] R. W. Davidge and A. G. Evans, "The strength and fracture of stoichiometric polycrystalline UO_2", J. Nucl. Mater., vol. 33, pp. 249–260, 1969.

[3] J. M. Gatt, J. Sercombe, I. Aubrun, and J. C. Ménard, “Experimental and numerical study of fracture mechanisms in UO_2 nuclear fuel”, Eng. Fail. Anal., vol. 47, no. PB, pp. 299–311, 2015.
[4] H. Sonnenburg, W. Wiesenack, J. K.-H. Karlsson, A. Alvestav, “Report on fuel fragmentation, relocation and dispersa“, OECD, NEA/CSNI/R/2016.
[5] F. Lemoine, “High burnup fuel behavior related to fission gas effects under reactivity initiated accidents (RIA) conditions”, J. Nucl. Mater., Vol. 248, 1997, pp 238-248.
[6] S. Yagnick, J.A. Turnbull, J. Noirot, *C.* Walker, L. Hallstadius, N.Waeckel, P.Blanpain, “An Investigation into Fuel Pulverization with Specific Reference to High Burn-up LOCA”, 2014, JRC91476
[7] J.A. Turnbull, S. Yagnik, M. Hirai, M. D. Staicu, C. Walker, “An assessment of the fuel pulverization threshold during LOCA-type temperature transients”, 2015, JRC90645.
[8] I. Guénot-Delahaie *et al.*, “Simulation of reactivity-initiated accident transients on UO_2-M5® fuel rods with ALCYONE V1.4 fuel performance code”, *Nucl. Eng. Technol.*, vol. 50, n° 2, p. 268-279, 2018.
[9] T. R. G. Kutty, K. N. Chandrasekharan, J. P. Panakkal, and J. K. Ghosh, “Fracture toughness and fracture surface energy of sintered uranium dioxide fuel pellets”, J. Mater. Sci. Lett., vol. 6, no. 3, pp. 260–262, 1987.
[10] J. Spino, K. Vennix, and M. Coquerelle, “Detailed characterisation of the rim microstructure in PWR fuels in the burn-up range 40-67 GWd/tM”, J. Nucl. Mater., vol. 231, pp. 179–190, 1996.
[11] D. M. Frazer, “Elevated Temperature Small Scale Mechanical Testing of Uranium Dioxide”, UC Berkeley Thesis 2018.
[12] R. Henry, T. Blay, T. Douillard, A. Descamps-Mandine, I. Zacharie-Aubrun, J.M. Gatt, C. Langlois, S. Meille, “Local fracture toughness measurements in polycrystalline cubic zirconia using micro-cantilever bending tests”, Mech. Mater., vol. 136, no March, p. 103086, 2019.
[13] R. Henry *et al.*, “Irradiation effects on the fracture properties of UO_2 fuels studied by micro-mechanical testing”, J. Nucl. Mater., vol. 536, p. 152179, 2020.
[14] R. Henry *et al.*, “Fracture properties of an irradiated PWR UO_2 fuel evaluated by micro-cantilever bending tests”, J. Nucl. Mater., p. 152209, 2020.
[15] G. D. Quinn and R. C. Bradt, “On the vickers indentation fracture toughness Test”, in Journal of the American Ceramic Society, 2007, vol. 90, no. 3, pp. 673–680.
[16] D. B. Marshall *et al.*, “The compelling case for indentation as a functional exploratory and characterization Tool”, J. Am. Ceram. Soc., vol. 98, no. 9, pp. 2671–2680, 2015.
[17] J. Noirot, I. Zacharie-Aubrun, T. Blay, “Focused ion beam–scanning electron microscope examination of high burn-up UO_2 in the centre of a pellet”, Nucl. Eng. Technol., vol. 50, n°2, p. 259-267, 2018.
[18] J. Noirot *et al.* , “High burnup changes in UO_2 fuels irradiated up to 83 GWd/t in M5® claddings”, Nucl. Eng. Technol., vol. 41, no. 2, pp. 155–162, 2009.
[19] J. Noirot, L. Desgranges, et J. Lamontagne, “Detailed characterisations of high burn-up structures in oxide fuels”, J. Nucl. Mater., vol. 372, no 2-3, p. 318-339, 2008.
[20] ISO 13383-1:2012, “Fine ceramics (advanced ceramics, advanced technical ceramics) – Microstructural characterization – Part 1: Determination of grain size and size distribution”
[21] B. Michel, J. Sercombe, G. Thouvenin, et R. Chatelet, “3D fuel cracking modelling in pellet cladding mechanical interaction”, Eng. Fract. Mech., vol. 75, no 11, p. 3581-3598, 2008.
[22] J. M. Gatt, Y. Monerie, D. Laux, et D. Baron, “Elastic behavior of porous ceramics: Application to nuclear fuel materials”, J. Nucl. Mater., vol. 336, n° 2-3, p. 145-155, 2005.
[23] M. Marchetti *et al*., “Physical and mechanical characterization of irradiated uranium dioxide with a broad burnup range and different dopants using acoustic microscopy”, J. Nucl. Mater., vol. 494, p. 322-329, 2017.
[24] G. R. Anstis, “Indentation and fracture toughness I”, Transformation, vol. 46, no. September, pp. 533–538, 1981.

[25] K. Niihara, R. Morena, and O. Metals, “Evaluation of K_{ic} of brittle solids by the indentation method with low crack-to-indent ratios”, J. Mater. Sci. Lett., vol. 1, pp. 13–16, 1982.
[26] M. T. Laugier, “Palmqvist indentation toughness in WC-Co composites”, J. Mater. Sci. Lett., vol. 6, no. 8, pp. 897–900, 1987.
[27] D. Casellas, J. Caro, S. Molas, J. M. Prado, and I. Valls, “Fracture toughness of carbides in tool steels evaluated by nanoindentation”, Acta Mater., vol. 55, no. 13, pp. 4277–4286, 2007.
[28] D. Ćorić, M. Majić Renjo, and L. Ćurković, “Vickers indentation fracture toughness of Y-TZP dental ceramics”, Int. J. Refract. Met. Hard Mater., vol. 64, pp. 14–19, 2017.
[29] ASTM C1327-03, Norme Internationale, “Standard Test Method for Vickers Indentation Hardness of Advanced Ceramics”.
[30] ISO 4516, 1980, Norme Internationale, ”Revêtements métalliques – Essais de micro-dureté Vickers et Knoop”.
[31] Hj Matzke, “Indentation fracture and mechanical properties of ceramic fuels and glasses ”, Harwood, 1987.
[32] J. Spino, J. Cobos-Sabate, and F. Rousseau, “Room-temperature micro-indentation behaviour of LWR-fuels, part 1: Fuel microhardness”, J. Nucl. Mater., vol. 322, no. 2–3, pp. 204–216, 2003.
[33] R. McDonald, “An Evaluation of the Mechanical Properties and Microstructure in Uranium Dioxide Doped with Oxide Additives”, Thesis Arizona State University, 2014.
[34] H. Xiao, X. Wang, C. Long, Y. Liu, A. Yin, and Y. Zhang, “Investigation of the mechanical properties of ZrO_2-doped UO_2 ceramic pellets by indentation technique,” J. Nucl. Mater., vol. 509, pp. 482–487, 2018.
[35] N.J. Petch, “The cleavage strength of polycrystals”, The Journal of the Iron and Steel Institute 173 (5) (1953) 25-28.
[36] K. A. Terrani, M. Balooch, J. R. Burns, Q. B. Smith, “Young’s modulus evaluation of high burnup structure in UO_2 with nanometer resolution “, J. Nucl. Mater., vol. 508, p. 33-39, 2018.
[37] J. P. Best *et al*., “A comparison of three different notching ions for small-scale fracture toughness measurement”, Scr. Mater., vol. 112, pp. 71–74, 2016.
[38] B. N. Jaya, C. Kirchlechner, and G. Dehm, “Can microscale fracture tests provide reliable fracture toughness values ? A case study in silicon”, J. Mater. Res., vol. 30, no. 5, 2015.
[39] A. Doitrand, R. Henry, I. Zacharie-Aubrun, J.-M. Gatt, et S. Meille, “UO_2 micron scale specimen fracture: Parameter identification and influence of porosities”, Theor. Appl. Fract. Mech., vol. 108, 2020.
[40] B. Gong, D. Frazer, T. Yao, P. Hosemann, M. Tonks, et J. Lian, “Nano- and micro-indentation testing of sintered UO_2 fuel pellets with controlled microstructure and stoichiometry”, J. Nucl. Mater., vol. 516, p. 169-177, 2019.May, p. 102665, 2020.
[41] France. Commissariat à l’énergie atomique, “Les Combustibles nucléaires”, Une monographie de la Direction de l’Energie Nucléaire, Commissariat à l'énergie atomique (CEA) - Collection E-den, 2008.
[42] T. Wiss *et al*., “Evolution of spent nuclear fuel in dry storage conditions for millennia and beyond”, J. Nucl. Mater., vol. 451, no 1-3, p. 198-206, 2014.
[43] E. Federici, A. Courcelle, P. Blanpain, et H. Cognon, “Helium production and behavior in nuclear oxide fuels during irradiation in LWR”, Am. Nucl. Soc. - 2007 LWR Fuel Performance/Top Fuel, p. 664-673, 2007.